



## Ceramic Waste Powder as a Partial Substitute of Fly Ash for Geopolymer Concrete Cured at Ambient Temperature

Jay K. Bhavsar <sup>1\*</sup> , Vijay Panchal <sup>1</sup>

<sup>1</sup> M. S. Patel Department of Civil Engineering, Chandubhai S. Patel Institute of Technology, Charotar University of Science and Technology, Changa, Anand, Gujarat 388421, India.

Received 16 February 2022; Revised 19 June 2022; Accepted 25 June 2022; Published 01 July 2022

### Abstract

The growth of the construction industry has expanded the demand for ceramic building products such as ceramic tiles, which constitute essential building materials. Nonetheless, a huge quantity of waste powder is produced during the polishing of ceramic tiles. The disposal of ceramic waste powder is a key environmental concern that needs to be properly addressed. The purpose of this research is to evaluate the potential of recycling ceramic waste powder as a geopolymer binder. The main objective consists of exploring the impacts of two types of ceramic waste powder (vitrified tiles and wall tiles) on the partial substitution of fly ash in geopolymer concrete. For this, concrete was prepared under ambient conditions without oven curing. Slump, compressive strength, split tensile strength, and modulus of elasticity tests were performed to measure the workability and the mechanical properties of the geopolymer concrete. Its durability was evaluated through water absorption and sorptivity tests. The microstructural behavior was investigated using scanning electron microscopy and X-ray diffraction measurements. The investigation revealed that a 15% partial replacement of fly ash by wall-tile ceramic waste powder in geopolymer concrete gave similar compressive strength, a 3% increase in tensile strength, and a 7% improvement in the modulus of elasticity. Partial replacement of fly ash with 15% vitrified ceramic waste powder reduced sorptivity and improved the microstructure of geopolymer concrete. The findings revealed that ceramic waste powder can be used to replace 10–15% of the fly ash in M35 grade structural geopolymer concrete, which can be cured under ambient conditions.

*Keywords:* Sorptivity; Modulus of Elasticity; Water Absorption; Ceramic Waste Recycling.

### 1. Introduction

The concrete industry is now moving toward the development of sustainable concrete using industrial by-products for partial replacement of cement. The use of industrial wastes in geopolymer concrete (GPC) facilitates waste recycling and promotes the production of eco-friendly concrete [1]. Fly ash geopolymer has been used as a substitute for Portland cement owing to its availability, low water demand, and low CO<sub>2</sub> emissions, [2, 3], essentially as a recycled geopolymer binder [4, 5]. Materials with high aluminosilicate compositions, such as fly ash, slag, and meta-kaoline, produce geopolymers with alkali content [6, 7], where NaOH, KOH, and Na<sub>2</sub>SiO<sub>3</sub> are commonly used in most studies [8]. Polycondensation helps aluminosilicate materials form geopolymer gels. Thus, geopolymer produces concrete that is as firm as Portland cement concrete. Heat curing has a vital influence on GPC properties, which has been used from 40 to 85 °C for geopolymerization reactions [9]. Bakria et al. found an optimum GPC temperature of 60 °C [10]. Nonetheless, the heat curing is hindering the use of GPC in regular applications due to its demanding energy budget. Thus, current research efforts are being made toward the development of GPC that can be cured at an average room temperature.

\* Corresponding author: [jaybhavsar.cv@charusat.ac.in](mailto:jaybhavsar.cv@charusat.ac.in)

 <http://dx.doi.org/10.28991/CEJ-2022-08-07-05>



© 2022 by the authors. Licensee C.E.J, Tehran, Iran. This article is an open access article distributed under the terms and conditions of the Creative Commons Attribution (CC-BY) license (<http://creativecommons.org/licenses/by/4.0/>).

The ceramic industry generates huge amounts of ceramic waste powder (CWP) during tile grinding and polishing processes [11]. Approximately 8 to 12% of the total waste is generated during the tile glazing and polishing processes [12]. This waste is discarded inland, causing ground, water, and air pollution in the surrounding environment [13]. CWP contains high amounts of silica and alumina; some are reactive [14] and constitute suitable source materials for GPC.

Many researchers have replaced cement with CWP to create cement-based concrete. The M25 grade of self-compacting concrete (SCC) was developed by Dieb et al., incorporating CWP as a cement substitute with an optimum percentage of 10–20% of cement. CWP showed better segregation resistance than ground granulated blast furnace slag (GGBS)-based SCC [13]. However, the use of CWP in GPC is reported to be significantly lower. Huseien et al. prepared an alkali-activated (AA) self-compacting concrete (SCC) using CWP and GGBS. The flow and passing ability of the concrete increased and the segregation resistance decreased with increasing CWP. The addition of CWP as a replacement for GGBS in alkali-activated SCC improves its resistance to sulfuric acid [15].

Aly et al. [16] examined the potential of using CWP in geopolymer concrete by using mortar specimens. The effects of air- and water-curing at 60 °C were investigated. Mixing with 40% slag and 60% CWP achieved 40 MPa strength after seven days. A high percentage of superplasticizer (4%) was used for flowability. The authors reported that CWP has excellent potential for use in GPC applications. Rashad and Essa [17] developed alkali-activated pastes with slag and CWP, which they cured under ambient conditions in a hot environment at 45 °C. The paste strength was increased when CWP was used to replace 0 to 50% of the slag in alkali-activated slag paste. The negative effect on flowability with an increase in CWP level is acknowledged. Zhang et al. [18] developed an AA paste with slag, fly ash, and ceramic waste. The samples were oven-cured at  $45 \pm 2$  °C. The different pastes were tested under thermal exposure for 2 h. The use of 20% CWP showed the highest strength after curing and thermal exposure.

Shoaei et al. [19] prepared geopolymer mortars using waste ceramic powder. The samples were designed with different alkaline liquid-to-binder ratios (A/B) and cured at temperatures varying from 60 to 105 °C. The highest strength (27.5 MPa) is achieved at 105 °C. The optimum mixture was cured at 90 °C with a 0.6 A/B. The flow of mortar improved with an increase in the A/B. Huseien et al. [20] used fly ash to replace GGBS in AA mortar made with CWP. The acid and sulfate attacks on the mortar reduced with a higher fly ash quantity. In another study, the use of red ceramic waste was reported as a substitute binder for a metakaolin-based geopolymer mortar developed at 60 °C oven curing. A reduction in the compressive strength (CS) accompanied by an improvement in particle packing with partial replacement of red ceramic waste were reported [21]. Metakaolin was replaced by ceramic waste and found to be suitable for producing geopolymer roof tiles. A longer duration is necessary to produce tiles at ambient temperature [22]. Saxena and Gupta (2022) recommended five percent ceramic waste as a replacement for fly ash for 60 °C oven-cured GPC. The properties of GPC with 5% CWP are found comparable to the reference mix [23]. The use of rice husk ash and ceramic dust as GPC binders produced negative results on flow and water absorption. However, only ceramic dust replacement has shown positive effects on GPC [24].

Previous studies have reported that fly ash can be used to make GPC and avoid a high amount of slag. A higher quantity of slag yields calcium-based reaction products and a lower amount of geopolymer gel. Previous studies have reported class F fly ash with other binders for GPC under ambient conditions [6, 12, 25–30]. The method of heat curing limits the application of GPC in cast-in situ operation. The reactivity of fly ash was lower at room temperature, thus GGBS, nanosilica, carbon nanotubes, and alccofine were added as binders to enhance the reactivity of GPC at ambient temperature [25, 27, 29, 31].

The properties of concrete differ from those of mortar and paste. The mortar performance cannot replicate the exact performance of concrete. The aforementioned literature survey reports previous studies on geopolymer mortar or geopolymer paste incorporating CWP as a binder, mainly focusing on replacing GGBS with CWP. The majority of works reported oven-cured GPC. Simultaneously, the use of GGBS and CWP also requires a high quantity of admixture for workability, which may increase the cost of GPC. The long-term performance of AA slag could weaken, whereas the performance of fly ash GPC is more stable [32]. Shah and Huseien (2020) have recently reported on the improved performance of an AA mortar mixes (comprising a high quantity of CW and fly ash) against acid attacks and under high temperatures, compared to mortar consisting of high GGBS quantities [33].

The past decade has seen an increase in the use of ceramic products, which is expected to rise in the future. There is a need to identify multiple alternatives for recycling and using ceramic waste effectively. So far, very limited research has been carried out on CWP as a fly ash substitute for geopolymers. To the best of our knowledge, no work has been reported yet on the incorporation of CWP as a fly ash replacement in GPC with curing at ambient temperatures. The use of CWP as a substitute for fly ash in GPC prevents environmental degradation and preserves the valuable minerals used in cement manufacturing. More importantly, it effectively contributes to reducing the CO<sub>2</sub> release inferred by the manufacturing of the cement, which promotes concrete sustainability.

Hence, the current research aims at exploring the impact of CWP on low-calcium fly ash GPC developed during ambient curing, in which fly ash was selected as the prime source material and CWP was used as the substitute binder.

The ceramic wastes used here were polishing wastes, which further highly reduced energy consumption compared to the process of crushing ceramic tiles into a powder form. The main objectives of this study are twofold: preparing an economical, average-strength, and workable M35 grade GPC and identifying the optimum replacement of CWP for GPC. For this, two types of CWP were explored. A 100% fly ash-based GPC was prepared as the base mix, and CWP was used to replace 10, 15, and 20% of the fly ash. A lower A/B and ambient curing was used to minimize the cost of GPC. The experiments were performed at an ambient temperature of  $35 \pm 2^\circ\text{C}$ .

## 2. Materials and Methods

### 2.1. Research Methodology

Figure 1 explains the workflow diagram of the research procedure adopted.

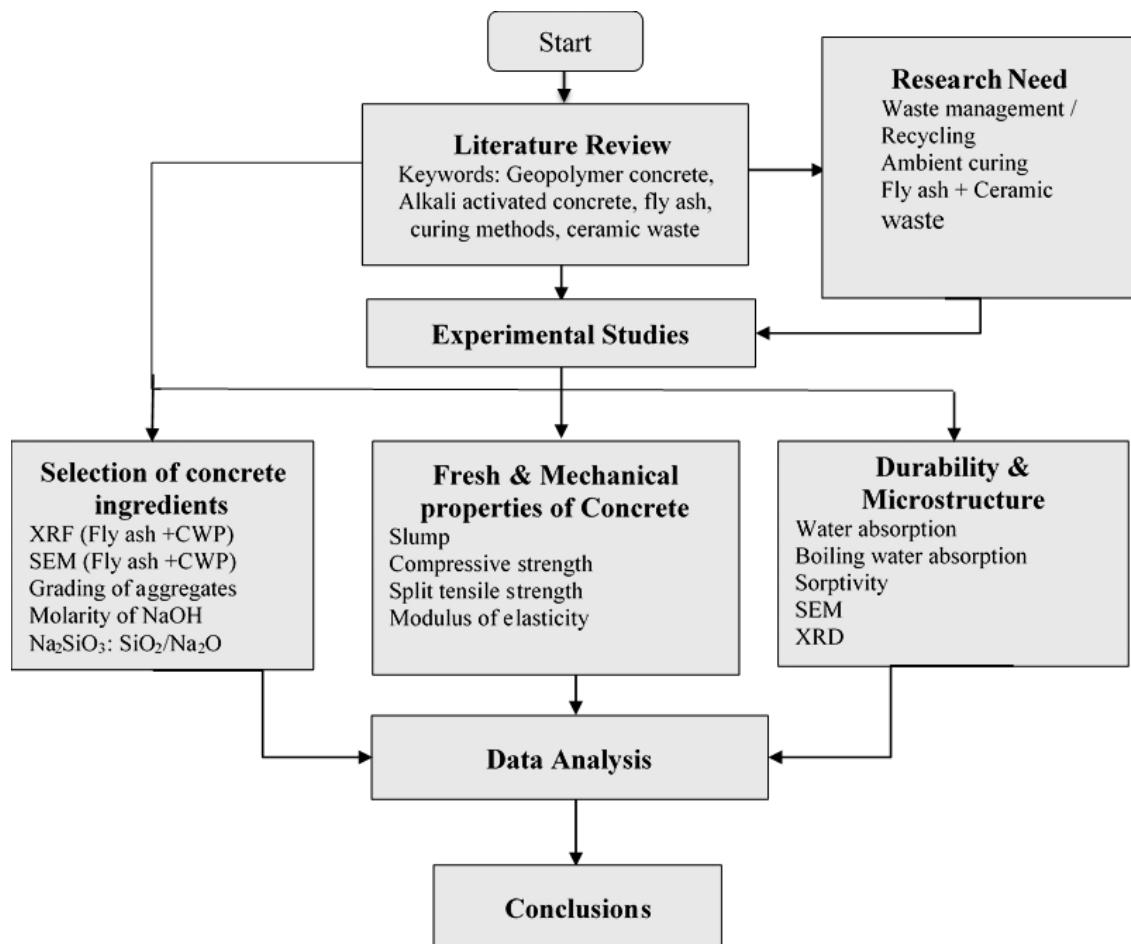


Figure 1. Research methodology diagram

### 2.2. Fly Ash

The fly ash was acquired from the Wankbori Thermal Plant, India. The results of a chemical analysis by X-ray fluorescence is summarized in Table 1. This result confirms the chemical necessity of fly ash used in concrete as per IS 3812-1:2013 [34]. The specific gravity of the fly ash was 2.71, and its surface area was  $5538 \text{ cm}^2/\text{g}$ . SEM imaging reveals a spherical shape particles microstructure in the fly ash, as shown in Figure 2. Owing to their spherical form, these micro-particle inclusions help improving the workability and decrease water demand.

Table 1. Chemical analysis of the binder (%)

Binder	SiO <sub>2</sub>	Al <sub>2</sub> O <sub>3</sub>	Fe <sub>2</sub> O <sub>3</sub>	CaO	MgO	Na <sub>2</sub> O	K <sub>2</sub> O	SO <sub>3</sub>	P <sub>2</sub> O <sub>5</sub>	TiO <sub>2</sub>
Fly ash	58.98	15.19	12.5	1.82	0.62	0.25	1.88	1.60	0.58	3.98
VCWP	70.71	11.56	2.86	3.45	1.21	1.39	3.39	0.46	0.17	1.48
WCWP	57.55	11.54	7.77	10.86	1.68	0.96	1.50	2.88	0.28	2.45

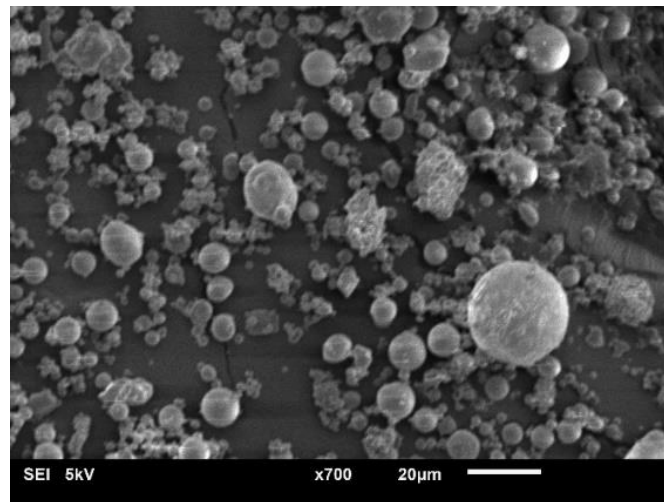
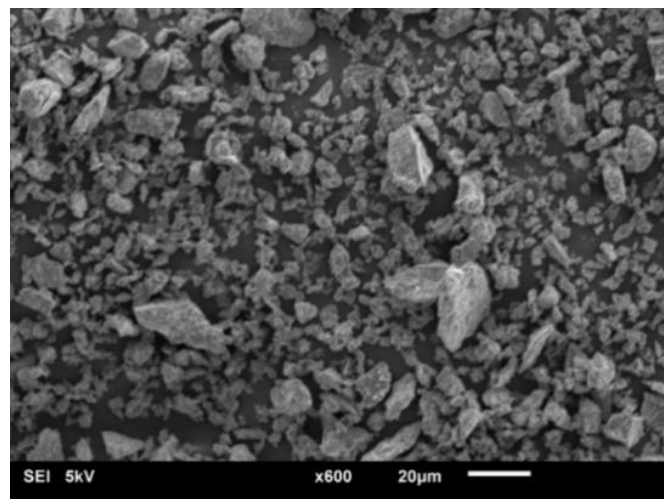


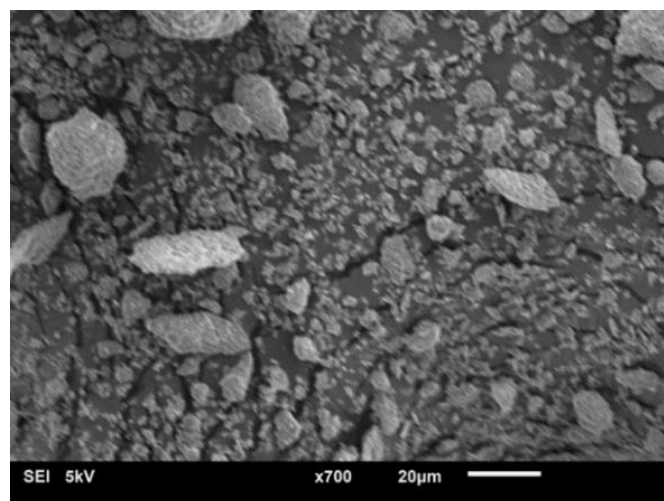
Figure 2. SEM image of fly ash

### 2.3. Ceramic Waste Powder

Two types of CWP were collected from the ceramic industry. Vitrified tile ceramic waste (VCWP) and wall-tile ceramic waste (WCWP) powders were used. Wastes were obtained during the polishing of ceramic tiles. The specific gravity of both VCWP and WCWP were 2.53. Their specific surface areas were  $4976 \text{ cm}^2/\text{g}$  and  $5778 \text{ cm}^2/\text{g}$ , respectively. Dieb et al. reported a  $5550 \text{ cm}^2/\text{g}$  surface area for CWP [35]. The chemical properties of both CWPs are described in Table 1. Both CWPs particles had angular shapes, as displayed shown in the SEM images in Figure 3.



(a)



(b)

Figure 3. SEM image (a) VCWP (b) WCWP

### 2.4. Activators

Commercially available technical-grade sodium hydroxide (NaOH) flakes were used in this study. Previous investigations found that high NaOH molarity increases strength. Kumar et al. [36] found that 14 molar (14 M) solution resulted in a higher compressive strength when blended geopolymer concrete was prepared. Hence, a NaOH 14 M solution was prepared by dissolving 404 g of flakes in 556 g of water. The concentrated NaOH solution was prepared 24 h prior the concrete mixing. Sodium silicate ( $\text{Na}_2\text{SiO}_3$ ) was purchased from the supplier at a 1.97  $\text{SiO}_2$  to  $\text{Na}_2\text{O}$  proportion by mass. The percentages of  $\text{SiO}_2$ ,  $\text{Na}_2\text{O}$ , and water in the  $\text{Na}_2\text{SiO}_3$  were 31.4, 15.9, and 52.7%, respectively.

### 2.5. Aggregates

Coarse aggregates (CA) (10- and 20-mm in size) were used in this experiment. The fine aggregates (FA) were smaller than 2 mm with a fineness modulus of 2.56 and Zone II as per the Indian standard (IS). FA and CA had specific gravity values of 2.6 and 2.69, respectively. Both aggregates were graded according to the requirements of IS 383:2016 [37]. The grading curve for FA and CA is presented in Figure 4.

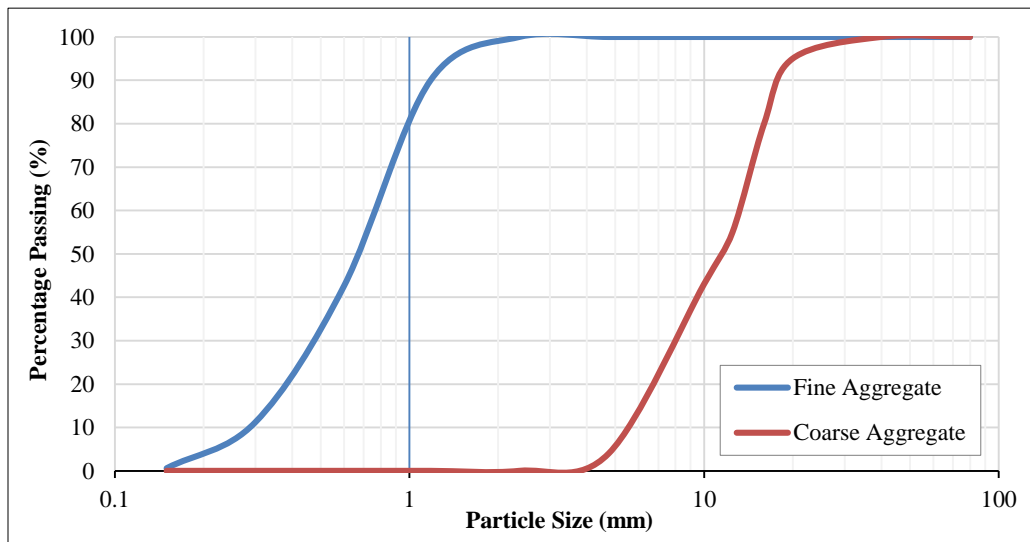


Figure 4. Grading of aggregates

### 2.6. Concrete Sample Preparation

The GPC mixes were designed by referring to a study by Lloyd & Rangan [38]. The anticipated GPC weight per square meter was  $2400 \text{ kg/m}^3$ . The proportions of FA and CA were considered to be 77% of the total mass of concrete. All mixtures had 0.35 A/B and a 2.5  $\text{Na}_2\text{SiO}_3/\text{NaOH}$  ratio. Additional water was added to form a workable concrete mix. Seven mixes were developed with a control mixture of fly ash GPC. The fly ash was partly substituted by VCWP and WCWP at 10%, 15%, and 20% by weight. The workability and target strength were experimentally determined.

Surface-Saturated Dry (SSD) aggregates were used to prepare concrete samples. The NaOH and  $\text{Na}_2\text{SiO}_3$  solutions were combined 30 min before concrete mixing, and the dry ingredients were mixed in a pan mixture for 1–2 min before adding the NaOH and  $\text{Na}_2\text{SiO}_3$  solutions. After 2–3 minutes of mixing, additional water was added and the concrete was mixed until the slurry was completely homogeneous. The total mixing period was 4–5 min. All the molds were filled with three layers of concrete and compacted for 2 min on a vibrator. After 24 h, the samples were demold and kept at room temperature. The final design mixes for the GPC are summarized in Table 2. The average results for the three specimens from different batches are reported for discussion.

Table 2. Geopolymer concrete mix ( $\text{kg/m}^3$ )

Mix no.	Mixtures	Aggregates		Binders			Alkaline Solution		Extra Water	Superplasticizer
		Coarse		Sand	Fly Ash	CWP	$\text{Na}_2\text{SiO}_3$	NaOH		
		20 mm	10 mm							
1	GC	610	406	832	408.88	-	102.22	40.89	41	-
2	GCV10	610	406	832	368.00	40.88a	102.22	40.89	41	-
3	GCV15	610	406	832	347.56	61.33a	102.22	40.89	41	-
4	GCV20	610	406	832	327.11	81.77a	102.22	40.89	53	6.13
5	GCW10	610	406	832	368.00	40.88b	102.22	40.89	41	-
6	GCW15	610	406	832	347.56	61.33b	102.22	40.89	41	-
7	GCW20	610	406	832	327.11	81.77b	102.22	40.89	53	6.13

Mixture: GC- Geopolymer Concrete, Vx-Percentage of VCWP, Wx- Percentage of WCWP, aVCWP, bWCWP

### 3. Fresh and Mechanical Properties

A slump test was performed to assess the fresh properties proposed mixes. It was performed in compliance with the IS 1199–2:2018 standard [39]. The slump behavior of all the measured samples was the true natural slump. Concrete with a shear or collapsible nature was rejected.

The compressive strength experiment was performed on a 2000 kN AIMIL digital compression testing machine (CTM), as per IS 516:1959 [40]. A constant load was applied at a pace-rate of 14 N/mm<sup>2</sup>/min. The testing periods were 3, 7, 28, and 56 days. The split tensile (ST) experiment was performed according to IS 5816:1999 [41]. The cylindrical specimen was maintained horizontally, as shown in Figure 5. This was examined after 28 days.



Figure 5. Tensile strength test

The Young's modulus (MOE) of GPC was evaluated as per the IS 516: 1959 standard procedure [40]. The experiment was performed by keeping the specimen vertically in the CTM. As indicated in Figure 6, a specimen was fitted with a longitudinal extensometer. The compression load was given at a rate of 14 N/mm<sup>2</sup>/min. The deformations at corresponding loads were measured using a dial gauge and CTM reading. A stress-strain curve was plotted, and the MOE was calculated by finding the slope of the stress-strain line. MOE of three specimens were measured after 56 days, and an average value is reported.



Figure 6. Test setup of MOE

### 4. Durability Performance

The water absorption (W.A) was determined using the ASTM C642–13 standard procedure [42]. The samples were dried in an oven at 110 °C for 24 h until a constant mass was obtained. Then, they were immersed in water at 23 °C for 48 h to regain their saturated weight. The dry weight of the specimen is denoted as (A) whereas the saturated weight of the specimen is referred to as (B). Equation 1 was used to determine the water absorption (W.A) percentage of each specimen. The samples were then immersed in boiling water for 5 h and allowed to cool for 15 h to a final temperature of 23 °C. The saturated weight of the boiled specimen is denoted as (C), and the water absorption of the boiled specimen (W.Ab) was calculated using Equation 2.

$$W.A = \frac{B-A}{A} \times 100 \quad (1)$$

$$W.Ab = \frac{C-A}{A} \times 100 \quad (2)$$

According to ASTM C 1585–13 [37], a water sorptivity test was performed on a cylindrical specimen. The samples were stored for three days at a  $(50 \pm 2)$  °C temperature and  $80 \pm 3\%$  relative humidity. All samples were stored in sealable containers for 15 days prior to testing. The sealing material was applied to the side surfaces. Figure 7 shows the sorptivity experimental setup. The specimens were placed in a tray on raised supports and water was filled 1–3 mm above the support. Sorptivity was obtained as the slope of a line plotted between the absorption ( $I$ ) versus time square root ( $\sqrt{t}$ ). “ $P$ ” was calculated from Equation 3.

$$I = \frac{mt}{a \cdot d}, \quad (3)$$

where  $I$  is the absorption,  $mt$  is change in mass of a specimen in grams, at time  $t$ ,  $a$  is area of the specimen in  $mm^2$ , and  $d$  is density of water  $g/mm^3$ .



Figure 7. Sorptivity test setup

SEM was carried out on paste samples of 5 mm diameter for the microstructural analysis of GPC. An alkaline solution with a  $Na_2SiO_3/NaOH$  ratio of 2.5 was used. Paste samples GP, GPV15, and GPW15 were prepared by replacing 15% fly ash with CWP. The samples were stored at ambient temperature for 56 d, and coated with platinum prior to SEM imaging. For comparison, all micro-images were captured at the same magnification and microscope voltage.

Paste samples of GP, GPV15, and GPW15 were crushed into fine powders for X-ray diffraction (XRD) analysis. The analysis was done at an age of 56 days, and crystalline phases were identified at  $2\theta$  angles from  $10^\circ$  to  $70^\circ$ .

## 5. Results and Discussion

### 5.1. Workability of GPC

The flow of GPC relies on the binder, water, and additives used. The developed GPC could be handled easily for two hours without any sign of setting whereas it hardens after 24 h of casting.

Figure 8 shows the slump values for the GPC mixtures. The slump values were significantly influenced by the CWP replacement, showing a decreasing trend as the percentage of CWP increased. The maximum slump was recorded for reference GPC with 100% fly ash. In comparison to the reference mix, the slump was reduced by 10%, 40%, and 70% for GCV10, GCV15, and GCV20, respectively. This was reduced by 50%, 30%, and 55% for GCW10, GCW15, and GCW20, respectively. When 10% fly ash was substituted with VCWP, the slump fall was acceptable at approximately 10%. For 15% replacement of VCWP and WCWP slump was reduced by 40% and 30%. With an increase in the CWP content to more than 15%, the concrete became stiff. Hence, a superplasticizer was necessary to improve the workability of mixtures GCV20 and GCW20. For these mixes, a 1.5% naphthalene-based superplasticizer was used to increase the workability. Despite the additional water and admixture in mixes GCV20 and GCW20, a lower slump was reported. The slump reduction was attributed to the high water absorption and angular shape (Figure 3) of the CWP particles [13]. The angular shape of the particles increases the friction between the particles, and hence, reduces the workability.

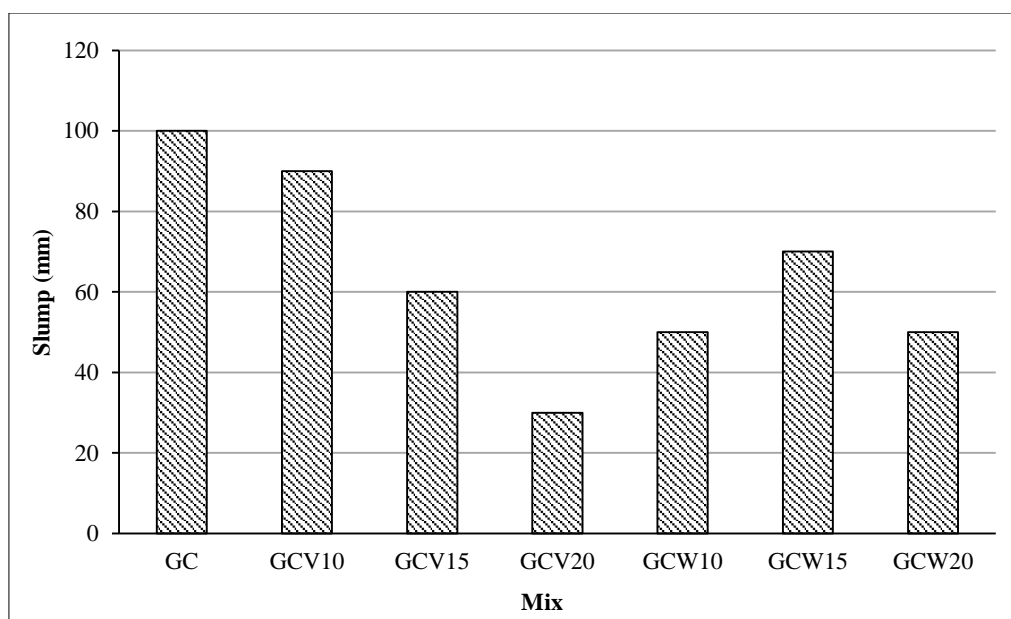


Figure 8. Slump results of GPC

Previous research has shown a negative trend for workability when CWP replacement increases with other binders in paste, mortar, and concrete mixes. [17, 23].

There are several ways to overcome the workability problems of GPC. This can be improved using a high water-to-binder ratio and admixture. Although the compatibility of traditional admixtures must be investigated. Shoaie et al. reported that the flow of CWP mortar could be enhanced by increasing the A/B, which ranges from 0.4 to 0.7 [19]. However, increasing the alkaline content may decrease the strength and increase the cost of GPC.

## 5.2. Mechanical Strength of GPC

The essential properties of GPC with incorporated CWP are described in Table 3.

Table 3. Mechanical properties

Mixtures	Density (kg/m <sup>3</sup> )	Cube Compressive Strength (MPa)				Tensile Strength (MPa)	MOE (MPa)
		28 d	3 d	7 d	28 d		
GC	2387	12.07	27.10	49.02	49.96	3.65	26414.00
GCV10	2395	10.86	26.99	45.95	44.00	3.69	25482.00
GCV15	2392	10.80	27.32	45.38	45.62	3.74	26545.33
GCV20	2319	2.87	9.88	26.07	32.68	1.29	21514.00
GCW10	2385	16.92	30.76	48.78	47.81	3.64	26043.33
GCW15	2379	10.91	29.42	43.84	49.96	3.78	28411.33
GCW20	2300	3.24	11.73	27.00	31.42	2.27	18661.00

Generally, a high-density concrete provides better strength and fewer voids. In this study, the densities of all designed mixtures ranged from 2300 to 2395 kg/m<sup>3</sup> (Table 3). The maximum reduction in density of GPC was observed in the mixture of GCV20 and GCW20, which was approximately 3%. The remaining mixtures exhibited similar density values. The evaluated density values matched the density of plain cement concrete specified by the IS 456:2000 standard [43]. Our findings corroborate with previous studies, which recorded GPC density values within the range of 2147 to 2463 kg/m<sup>3</sup> [3, 27, 30, 44]. A decrease in density with an increase in CWP was reported for geopolymer mortars [45].

Figure 9 represents the effects of compressive strength at varying ages. In comparison to control mix, compressive strengths at 56 d for GCV10, GCV15, and GCV20 were reduced by 11.92%, 9.69%, and 34.58%, respectively. Similarly, the strengths of GCW10, GCW15, and GCW20 were reduced by 4%, 0%, and 37.0%, respectively. GCW10 and GCW15 resulted in a greater early strength (7 d) and final strength (56 d) relative to GCV10 and GCV15.

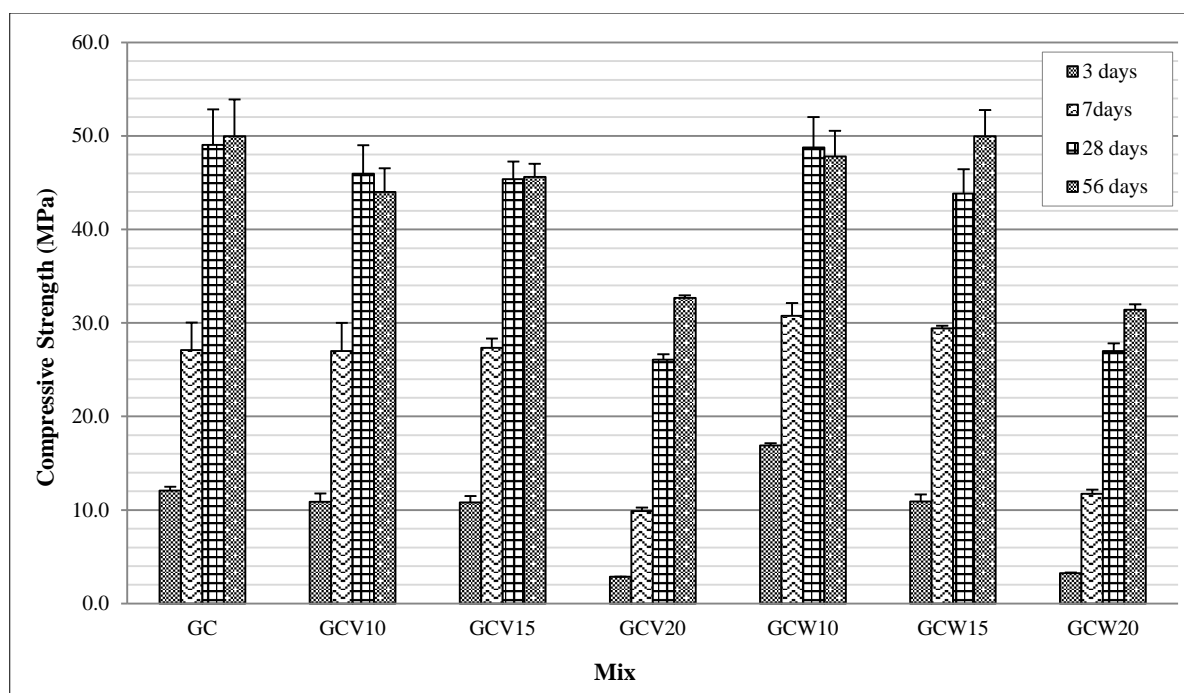


Figure 9. Compressive strength of GPC

The compressive strength of all mixtures improved gradually with age. This confirms the Geopolymerization process with increasing age [46]. GCW10 and GCW15 exhibited a high compressive strength due to the availability of 10% CaO (Table 1) in the WCWP, which resulted in tobermorite (CSH) gel at early stage. In addition, the compressive strengths at 28 and 56 d for GC, GCV10, GCV15, GCW10, and GCW15 were higher than the target strength (43.25 MPa) calculated as per the IS 10262:2019 standard, for the M35 grade concrete [47]. This implies that 15% CWP replacement with fly ash can produce M35 grade geopolymer concrete under ambient conditions. These designed mixtures (GC, GCV10, GCV15, GCW10, and GCW15) are appropriate for extreme exposure conditions, in agreement with IS 456:2000 [43]. The high water content and admixture increased the porosity of the GCV20 and GCW20 mixtures and reduced their density and compressive strength.

A lower mortar compressive strength with an increase in CWP as substitute of GGBS has been reported [15, 16, 48]. The decrease in the compressive strength of concrete could be attributed to the reduced lime percentage with the replacement of CWP with GGBS [15]. This validates the improvement in the compressive strength at an early days for GCW10 and GCW15. However, the percentage of CaO was very small; hence the 56-day strength was similar to that of the reference mix. In contrast, Rashad & Essa observed an improvement in the compressive strength of AA slag paste at 7 and 28 d, with an increase in CWP when replacing slag. The authors reported that hot climate conditions increased the geopolymerization rate and helped increase the strength at an early age [17]. In our present study, the high ambient temperature increased the rate of polymerization and resulted in a strength higher than 43 MPa at 28 days for 15% CWP replacement. Saxena and Gupta (2022) reported that a decrease in strength with increasing ceramic waste, disturbed the homogeneity of GPC owing to the angular shape of the ceramic waste [23].

The key factors for higher compressive strength at ambient temperature for reference mix and mix with 15% ceramic replacement are high surface area of binders, high ambient temperature, and presence of CaO in WCWP. The higher surface area of the binders and extended curing at room temperature can offer higher compressive strength of fly ash GPC [49]. Chindaprasirt and Rattanasak (2017) reported better later-age strength for fly ash GPC cured at 35 °C for 72 h compared to cure at 65 °C for 24 h [50]. An extended curing period improves the strength of ceramic dust-based geopolymer bricks. However, high curing temperature degrades the strength [51].

The values presented in Table 4 validate the experimental outcomes of compressive strength and imply that the average strength of GPC is achievable under ambient conditions. For comparison, the cube strength results of the study were converted into cylindrical strength. The strength gain process was frequently found slow in fly ash GPC at 28 d, taking a long time to complete geopolymerization. However, Saxena and Gupta (2022) reported a lower compressive strength than that in the present study because of oven curing. Also, different  $\text{Na}_2\text{SiO}_3/\text{NaOH}$  ratios, curing temperatures, and molarities of sodium hydroxide may result in a lower compressive strength.

**Table 4. Comparison of results with previous works**

Authors	Binders	Compressive Strength (MPa)	Curing condition	NaOH molarity	Na <sub>2</sub> SiO <sub>3</sub> /NaOH	Testing time (days)
Albatiar et al. [30]	Class F Fly ash	49.1	Ambient	14 M	0.6	90
Nath and Sarkar [3]	Class F Fly ash	33.1- 41.1	Ambient	14M	2.5	90
Vaidya et al [52]	Class F Fly ash	43.1	Ambient	Not reported	Not reported	28
Ngarm et al. [53]	Class C Fly ash	45.34,39.02	Ambient	15M	1.0,2.0	28
Saxena and Gupta [23]	Class F Fly ash + 5% CWP	18.8	1 day 60°C oven	Not reported	2	28
Present Study	Class F Fly ash + 10 - 15% CWP	35.2- 40	Ambient	14M	2.5	56

The split tensile strength (ST) is a vital property of concrete, whose results are presented in Figure 10. The results were compared with those of the control mix. Minor changes in ST, +1.16%, +2.63%, -0.12%, and +3.62% were observed for GCV10, GCV15, GCW10, and GCW15 mixtures, respectively. Replacement of CWP by 20% for GCV20 and GCW20 reduced the ST by 64% and 37%. A comparable ST was observed up to 15% CWP replacement. This implies that the recycling of 15% CWP as a fly ash substitute for GPC is plausible. In the past, the replacement of GGBS with CWP resulted in a low rate of chemical reaction and the formation of C-A-S- H gel [15]. However, in the present study, fly ash was replaced by CWP, and ST was not affected by a 15% CWP substitution. These results indicate that replacing CWP with fly ash has a more positive effect than replacing CWP with GGBS.

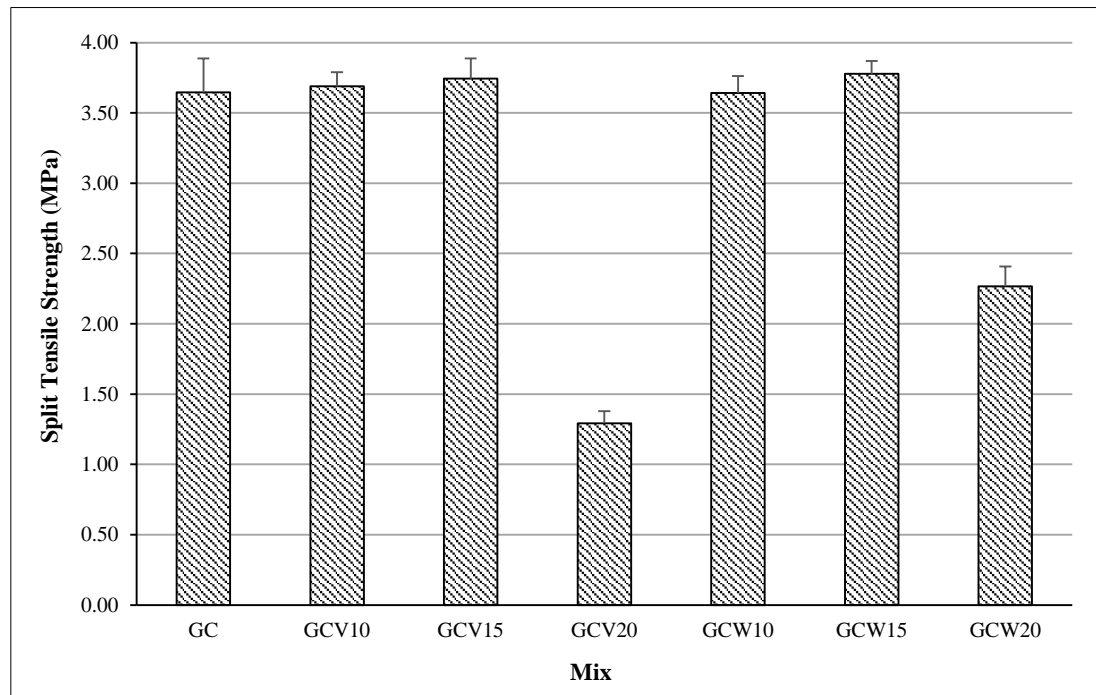


**Figure 10. Split tensile strength (28 days)**

Sofie et al. proposed Equation 4 to determine ST ( $f_{ctm}$ ) from the characteristic compressive cylinder strength of concrete ( $f_{ck}$ ) at 28 d with an experimental study carried out at 23 °C for fly ash and slag based GPC [44], whereas Lee and Shin proposed Equation 5 [54]. The relationship between ST and compressive strength in the present study is presented in Figure 11 and compared with the values obtained from Equations 4 and 5. Here, the 28-d cube strength was converted to cylindrical compressive strength as per IS 516:1959 [40]. The ST was slightly higher in the present study compared to previously reported works because of the differences in the curing temperature and binder composition [44, 54].

$$f_{ctm} = 0.3 \times f_{ck}^{2/3} \tag{4}$$

$$f_{ctm} = 0.47 \times f_{ck}^{0.52} \tag{5}$$

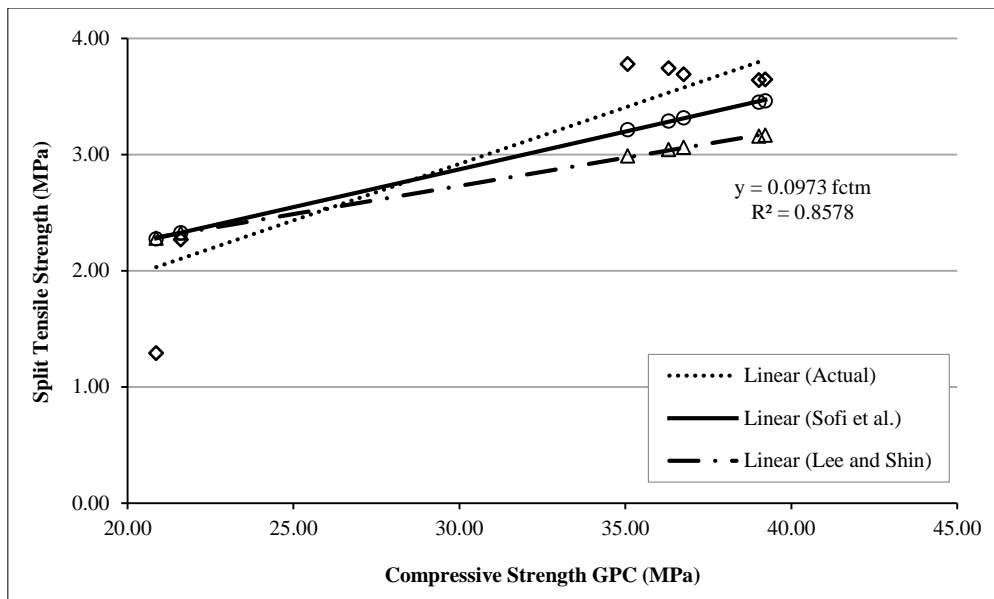


Figure 11. Compressive strength vs. ST strength in this work and previous studies

The modulus of elasticity (MOE) is an important property that must be consideration in the development of structural concrete. Figure 12 shows the MOE values obtained for different GPC at 56 days. The MOE decreased by 3.65% and 1.42% for GCV10 and GCW10, respectively, whereas it increased by 0.49% and 7% for GCV15 and GCW15, respectively. The MOE results for 15% CWP are equivalent to the reference GPC. The highest MOE was achieved for GCW15 among all mixtures, which is consistent with the compressive strength findings. The lime content of WCWP helped in the C-A-S-H gel creation and increased the MOE of GCW15. MOE values were reduced by 22.77% and 41.4% for GCV20 and GCW20, respectively, which is attributed to the extra water and superplasticizer creating more voids in GCV20 and GCW20.

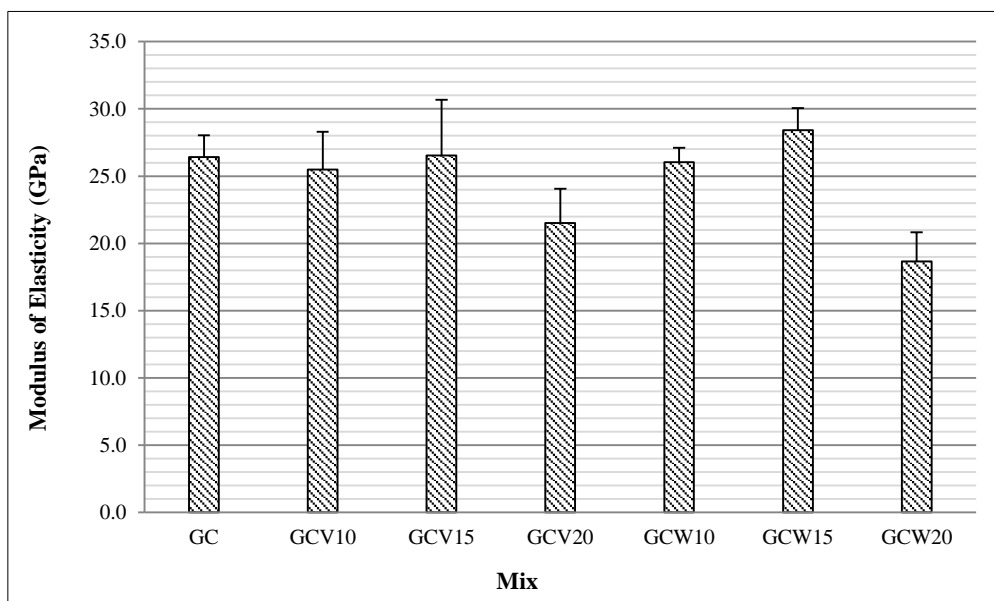


Figure 12. MOE of GPC (56 days)

Figure 13 displays the relationship between the MOE and the compressive strength obtained through Equations 6 to 8 given by IS 456:2000, Nath & Sarker, and Daiz-Loya et al. for fly ash GPC [3, 43, 55]. In the present work, the MOE of GPC was observed in the range of 26.41 to 28.41 GPa, which is lower than the MOE of plain cement concrete specified by IS 456:2000 [43]. Sofie et al. identified an MOE in the range of 23–39 GPa for fly ash GPC cured at 23 °C until testing [44]. The results of the present study match those proposed by Diaz-Loya et al. The present results are higher compared to those reported by Nath & Sarker due to the difference in ambient temperatures between the two studies. The comparison indicates that the MOE of fly ash GPC increases at a high ambient temperature of (35 ± 2) °C compared to that at 23 °C. A decrement in MOE was observed as the percentage of CWP increased for fly ash GPC made under oven curing [23, 27]. In addition, the MOE values reported by Saxsena and Gupta were high for lower

compressive strengths. This implies that temperature curing improves the MOE [23]. The MOE comparison with previous works suggests that the MOE of GPC depends on the compressive strength, curing temperature and curing time.

$$E = 5000\sqrt{f_{cc}} \tag{6}$$

$$E = 3510 \times f_{ck}^{0.5} \tag{7}$$

$$E = 0.037 \times \rho^{1.5} \times \sqrt{f_c} \tag{8}$$

where,  $f_{cc}$  is cube compressive strength,  $f_{ck}$  is compressive cylinder strength, and  $f_c$  is compressive cylinder strength after 3 d of curing at 60 °C for 3 d.

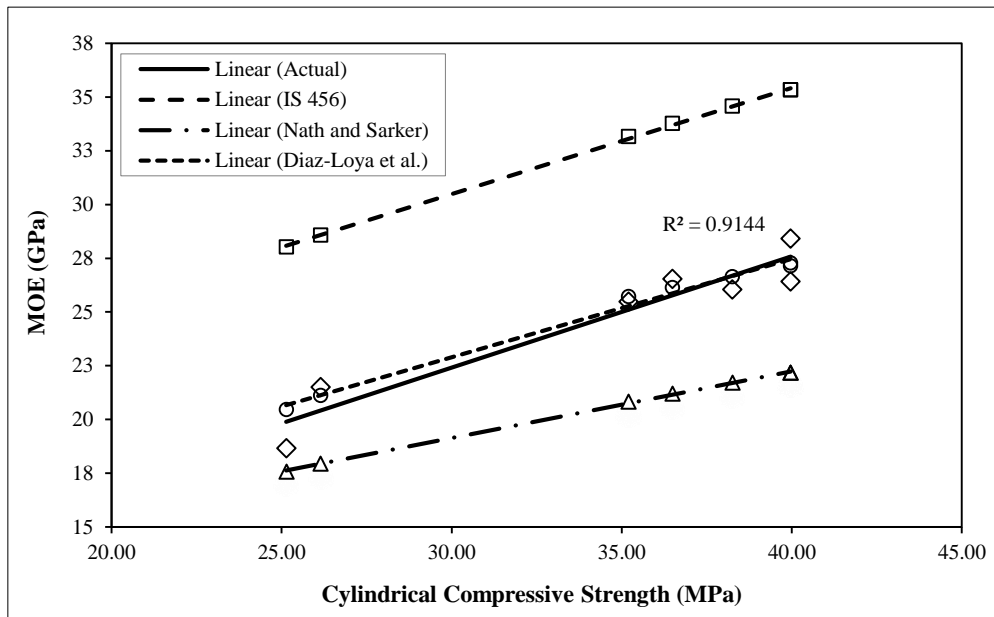


Figure 13. MOE vs. Compressive strength in this work and previously reported studies

### 5.3. Water Absorption

Water absorption (WA) provides an essential indication of the porosity and water tightness of concrete. Figures 14 and 15 show the percentage of WA after immersion in water at 23 °C and boiling temperature, respectively.

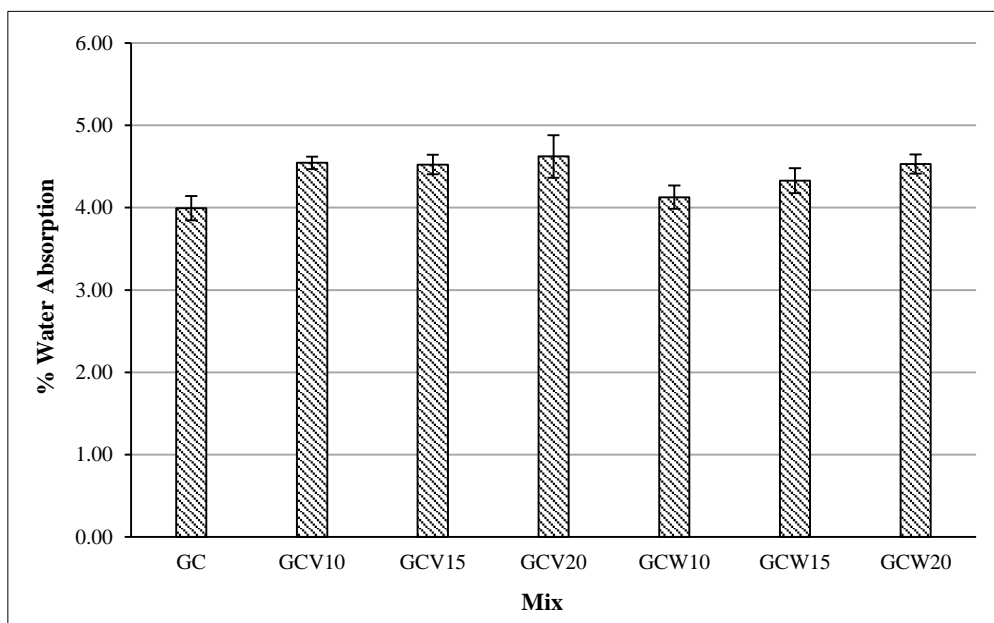


Figure 14. Water absorption after immersion in water

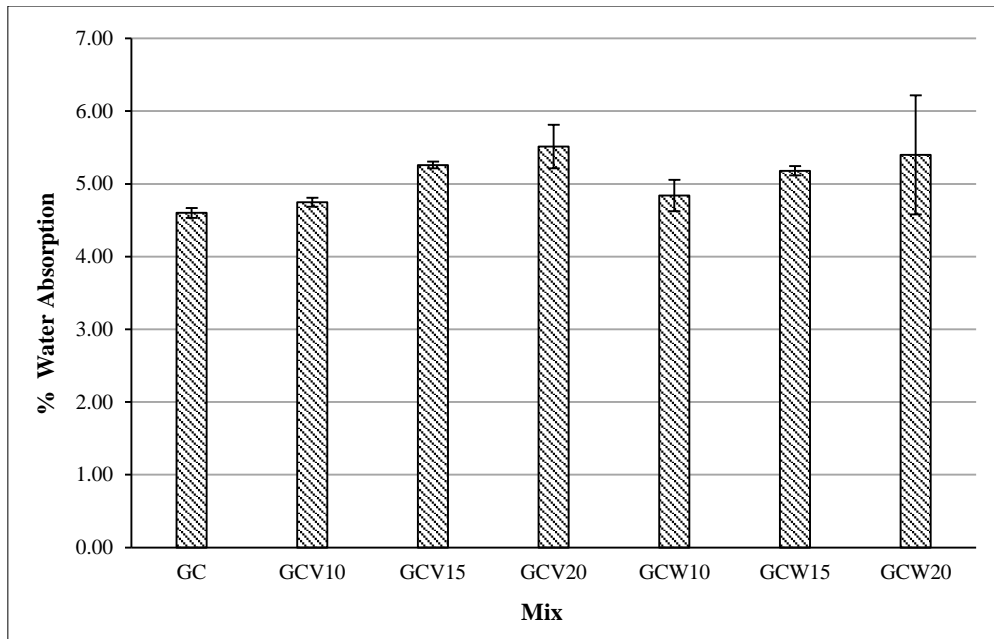


Figure 15. Water absorption after immersion in boiled water

Water absorption below 3% is considered a good durability indicator, while 3-5% is average, and more than 5% is considered as poor [56]. This study showed that WA increased with CWP, indicating that the porosity of GPC increases when CWP substitutes fly ash. However, it was below 5% for all mixes when the sample was immersed in water at standard temperature, and below 6% when the sample was immersed in boiling water. Previous studies have also reported an increase in WA with an increase in CWP as an alternative to fly ash or GGBS [15, 23].

5.4. Sorptivity

Aggressive ions are transported into the concrete through water. The sorptivity characterizes the transport mechanism of water into unsaturated concrete pores. It is an essential durability parameter for determining the microstructure and permeability of concrete. A lower sorptivity prevents the ingress of calcium and sulfate into concrete [57]. Figure 16 shows a sorptivity graph and Table 5 summarizes the corresponding sorptivity and R<sup>2</sup> values for each mix. GCV10, GCV15, and GCV20 showed lower sorptivity compared to GC, whereas the sorptivity values of GCW10 and GCW15 were slightly lower than that of GC.

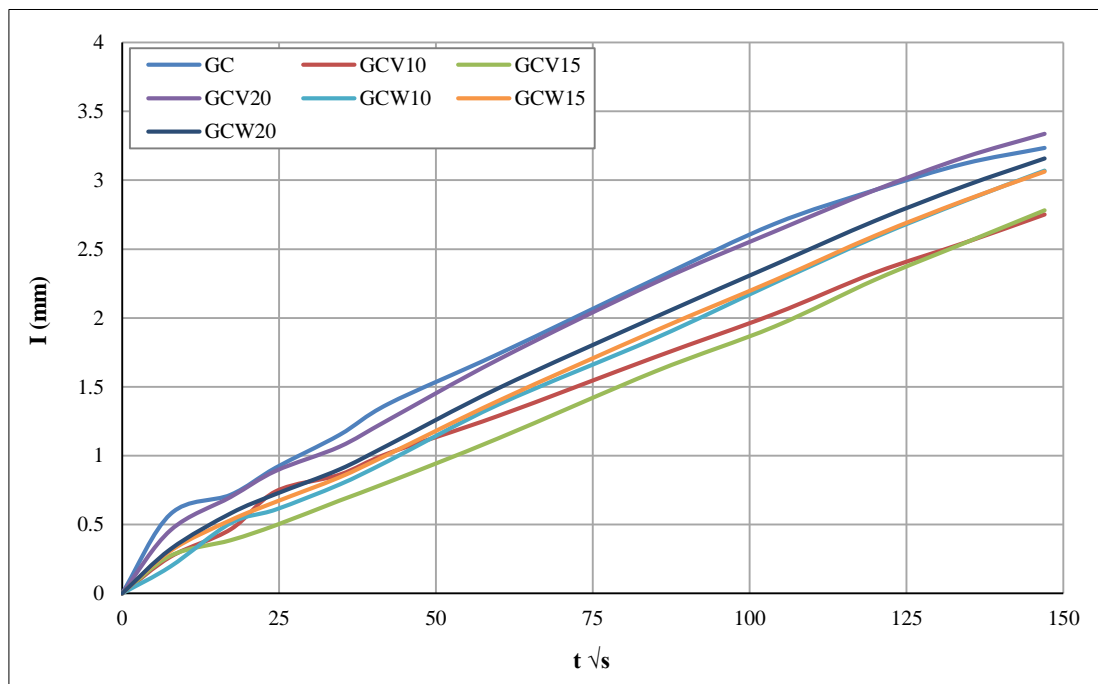


Figure 16. Initial rate of water absorption by capillary action

**Table 5. Sorptivity values for different mixtures**

Mix	S (mm <sup>1/2</sup> /s)	S (mm <sup>1/2</sup> /h)	R <sup>2</sup>
GC	0.0211	1.27	0.98
GCV10	0.0179	1.07	0.99
GCV15	0.0183	1.11	0.99
GCV20	0.0195	1.17	0.99
GCW10	0.0207	1.23	0.99
GCW15	0.0204	1.22	0.98
GCW20	0.0226	1.35	0.98

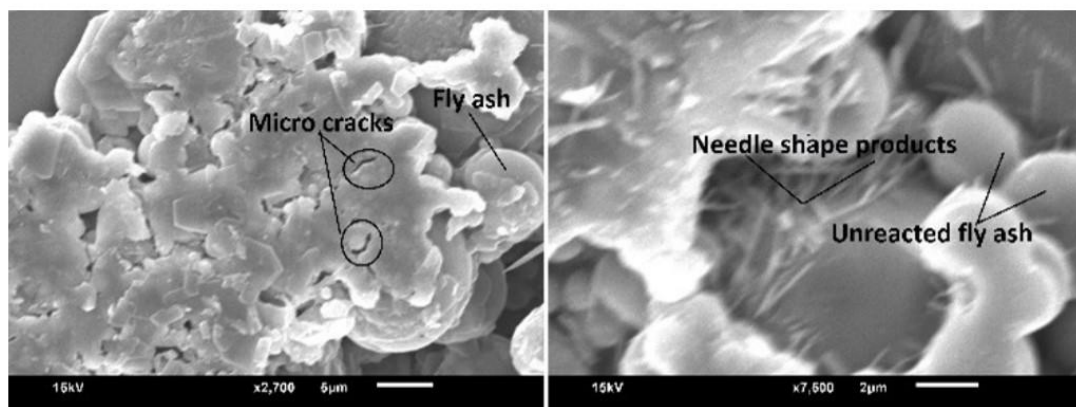
Table 6 shows the sorptivity index for concrete structure at early age, as proposed by Alexander et al [58]. It indicates that the sorptivity of the mixes designed in our study are excellent. Aly et al. [16] reported lower sorptivity for mortar samples when a 100% CWP mixture was used compared to a 60% CWP and 40% GGBS mixture. Another concrete based study on recycled aggregate concrete showed 10% replacement of CWP with cement reduces the sorptivity [59]. The impermeability of the concrete is improved with the addition of CWP in place of cement [11]. The reason for reduction in sorptivity is the influence of CWP on the reactivity and alteration in the pore structure.

**Table 6. Sorptivity Index**

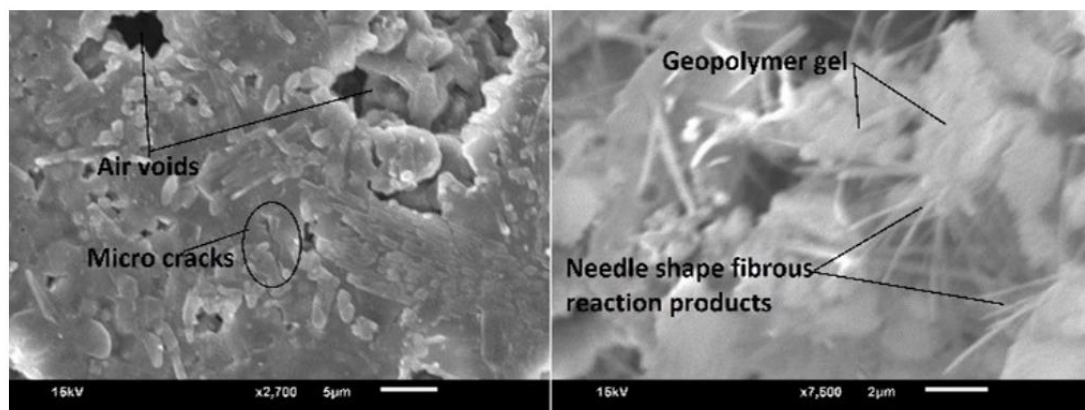
S (mm <sup>1/2</sup> /h)	Durability class
<6	Excellent
6-10	Good
10-15	Poor
>15	Very Poor

**5.5. Microstructure Analysis**

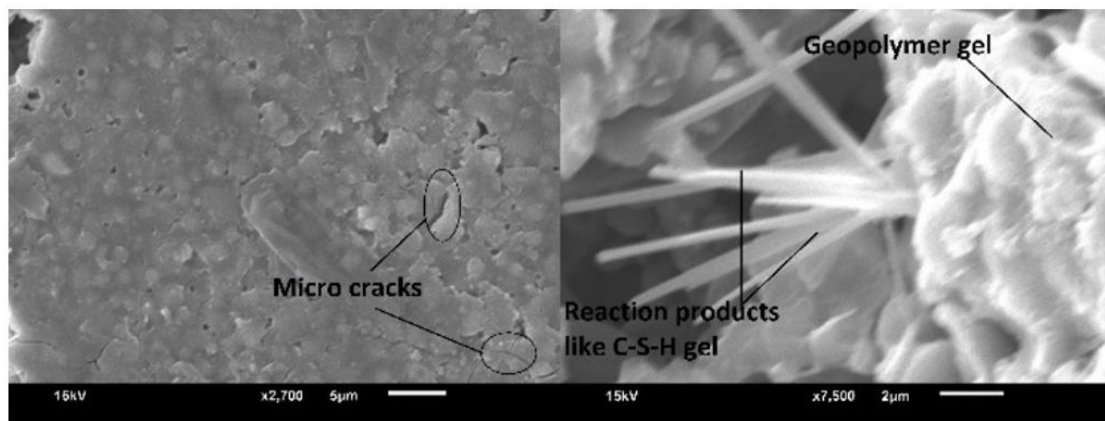
Figure 17 shows SEM images of the paste specimens for GP, GPV15, and GPW15. The paste microstructure includes unreacted particles, voids, and geopolymer gel [60].



(a)



(b)



(c)

Figure 17. SEM image (a) GP (b) GPV15 (c) GPW15

Figure 17-a shows an SEM image of GP revealing unreacted fly ash particles, voids, micro cracks, and geopolymer gels. It also shows small 2 µm needle-shaped products above the unreacted fly ash particles, which could be possibly attributed to zeolites that have developed as secondary products [26]. Figure 17-b shows the image of GPV15, which has a compact surface microstructure, voids, and needle-shaped reaction products with a fully developed geopolymer gel, which indicates the improvement in pore structure with the use of VCWP in fly ash geopolymers. A compact microstructure was also observed for GPW15 (Figure 17-c). This compactness was attributed to the high compressive strength and formation of the C-A-S-H phase. The combination of CWP may increase the compactness of the paste, and the remaining CWP can seal the paste voids [17, 18, 21].

A similar behavior was observed through a sorptivity test of the GCV10 and GCV15 mixes. However, unreacted SiO<sub>2</sub> increases porosity and degrades compressive strength [15]. In the paste matrix, the voids were not interconnected, and they improved the impermeability; hence, the compressive strength was decreased, while the impermeability and microstructure were enhanced. Figure 17-c shows an image of GPW15 with a product similar to that of the C-S-H gel. This confirms the formation of a C-A-S-H gel along with an N-A-S-H gel in the GPW15 [15]. This helped to improve the early compressive strength and high MOE.

### 5.6. XRD Analysis

Figure 18 shows the XRD patterns for the binders, indicating amorphous humps between 2θ values of 15°- 30°, 20°- 30° and 23°- 32° for fly ash, VCWP, and WCWP, respectively. The peaks of the fly ash and VCWP show the crystalline phases of quartz, mullite, and merwinite, whereas those of the WCWP show other phases, such as aluminium, nepheline, and calcite, with quartz and mullite.

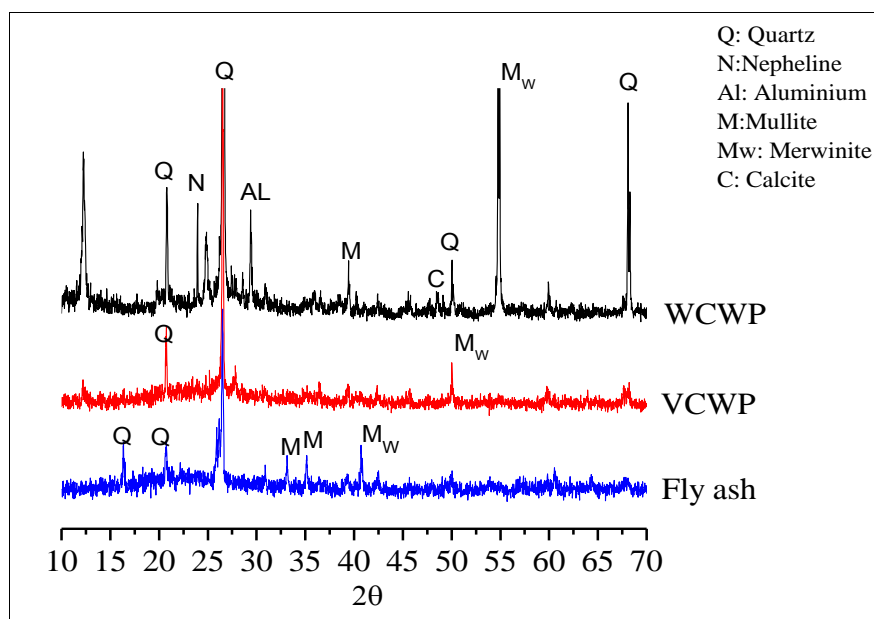


Figure 18. XRD of fly ash, VCWP, and WCWP

Figure 19 shows well-developed crystalline peaks of quartz at  $2\theta$  angles of  $16^\circ$ ,  $20.7^\circ$ , and  $26.5^\circ$  for all three diffraction patterns of GP, GPV15, and GPW15, respectively. The peaks of mullite were found in the patterns of GP and GPW15 between  $32^\circ$ – $35^\circ$ . Peaks that were not present on the VCWP pattern were also absent on that of the GPV15. Similar quartz and mullite phases have also been reported in GPs [26, 29, 60].

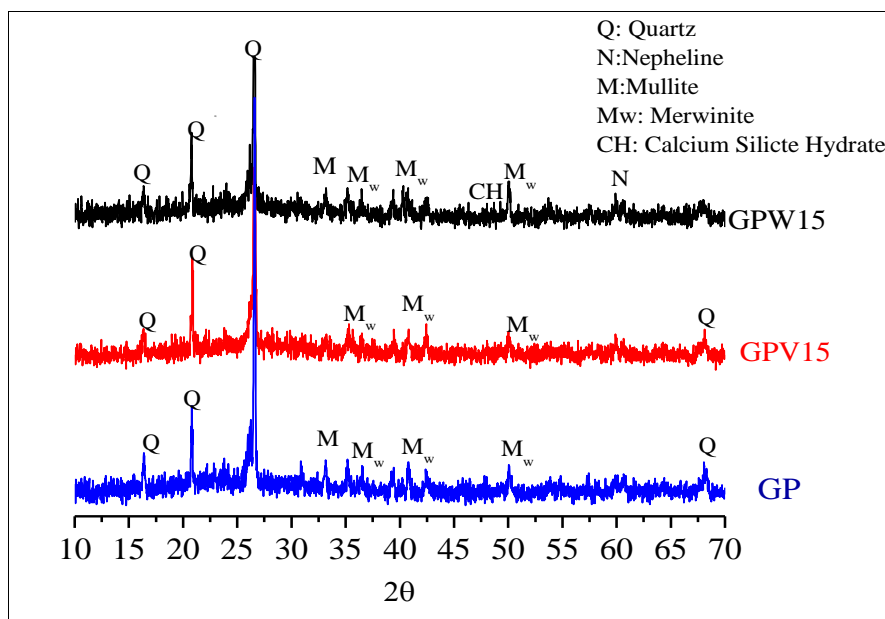


Figure 19. XRD of GP, GV-15, and GW-15

Most of the identified crystalline phases were similar to those observed in the source materials. This result indicates that the geopolymer gel is amorphous and is produced by the reaction of the source materials with the alkaline liquid [60]. The pattern of GW-15 shows the C-S-H gel phase and nepheline development, and similar phases have also been reported in other studies [17, 29]. Rashad and Essa found that the intensities of quartz, nepheline, calcite, and mullite peaks increased as CWP increased [17]. The presence of calcite in the WCWP (Figure 18) transformed it into a C-S-H gel-like product (Figure 17-c), which was also confirmed by SEM analysis. The C-S-H phase did not appear in the GP and GV-15 diffraction patterns because of the missing lime content.

## 6. Conclusions

The study explored the changes in the early and later age compressive strength of GPC by incorporating fly ash and CWP. The essential mechanical properties of GPC incorporating CWP were compared with those of IS 456:2000. Sorptivity testing revealed durability improvements with the use of CWP. Our findings contribute to the promotion of recycling VCWP and WCWP to produce fly ash GPC at ambient temperatures. The main conclusions of this study are summarized as follows:

- The crucial factors for the high performance of CWP and fly ash-based GPC are the high surface area of binders, extended ambient curing, the presence of lime, and optimum replacement of CWP. The optimum replacement may vary with changes in the curing temperature, curing time, properties of CWP, and the addition of other binders.
- The workability of GPC decreases with an increase in VCWP and WCWP in substitution of fly ash. The use of superplasticizers can further improve the workability, but the compatibility of the superplasticizer and its dosage needs to be determined.
- Compressive strength, split tensile strength, and MOE values for 15% replacement of the fly ash by CWP (VCWP and WCWP) are found appropriate for making an average-strength (35–45 MPa) GPC at ambient temperature ( $35 \pm 2$ ) °C without oven curing. This also suggests that 15% CWP can be utilized as a recycling binder in fly ash-based GPC.
- Replacing 15% of the fly ash with WCWP in GPC provides equivalent compressive strength, 3% higher split tensile strength, and 7% higher MOE. The replacement of fly ash with WCWP in GPC yielded a higher MOE than VCWP. Partial replacement of fly ash with 10–15% VCWP decreases the sorptivity and improves the compactness of fly ash GPC. The sorptivity performance of the VCWP replacement was better than that of the WCWP.
- The Young's modulus of fly ash and CWP-based GPC was lower than that mentioned in IS 456:2000. The equation suggested by Diaz-Loya et al. can be used to evaluate the MOE of fly ash and CWP-based GPC at ambient curing.

- SEM and XRD analyses confirmed the contribution of CWP to the polymerization process and the development of a better microstructure. This result revealed the presence of a C-A-S-H gel with an N-A-S-H gel owing to the replacement of fly ash by WCWP.

## 7. Declarations

### 7.1. Data Availability Statement

The data presented in study are available in the article.

### 7.2. Funding

The authors received no financial support for the research, authorship, and/or publication of this article.

### 7.3. Acknowledgements

The authors are thankful to the Charotar University of Science and Technology (India) for providing laboratory facilities for the research work.

### 7.4. Conflicts of Interest

The author declare no conflict of interest.

## 8. References

- [1] Saranya, P., Nagarajan, P., & Shashikala, A. P. (2019). Development of ground-granulated blast-furnace slag-dolomite geopolymers concrete. *ACI Materials Journal*, 116(6), 235–243. doi:10.14359/51716981.
- [2] Reddy, D. V., Edouard, J.-B., & Sobhan, K. (2013). Durability of Fly Ash–Based Geopolymer Structural Concrete in the Marine Environment. *Journal of Materials in Civil Engineering*, 25(6), 781–787. doi:10.1061/(asce)mt.1943-5533.0000632.
- [3] Nath, P., & Sarker, P. K. (2017). Flexural strength and elastic modulus of ambient-cured blended low-calcium fly ash geopolymer concrete. *Construction and Building Materials*, 130, 22–31. doi:10.1016/j.conbuildmat.2016.11.034.
- [4] Frayyeh, Q. J., & Kamil, M. H. (2021). The Effect of Adding Fibers on Dry Shrinkage of Geopolymer Concrete. *Civil Engineering Journal*, 7(12), 2099–2108. doi:10.28991/cej-2021-03091780.
- [5] Fernandez-Jimenez, A., García-Lodeiro, I., & Palomo, A. (2007). Durability of alkali-activated fly ash cementitious materials. *Journal of Materials Science*, 42(9), 3055–3065. doi:10.1007/s10853-006-0584-8.
- [6] Deb, P. S., & Sarker, P. K. (2017). Effects of Ultrafine Fly Ash on Setting, Strength, and Porosity of Geopolymers Cured at Room Temperature. *Journal of Materials in Civil Engineering*, 29(2), 6016021. doi:10.1061/(asce)mt.1943-5533.0001745.
- [7] Phoo-Ngernkham, T., Phiangphimai, C., Damrongwiriyunapap, N., Hanjitsuwan, S., Thumrongvut, J., & Chindaprasirt, P. (2018). A Mix Design Procedure for Alkali-Activated High-Calcium Fly Ash Concrete Cured at Ambient Temperature. *Advances in Materials Science and Engineering*, 2018, 1–13. doi:10.1155/2018/2460403.
- [8] Duxson, P., Fernández-Jiménez, A., Provis, J. L., Lukey, G. C., Palomo, A., & Van Deventer, J. S. J. (2007). Geopolymer technology: The current state of the art. *Journal of Materials Science*, 42(9), 2917–2933. doi:10.1007/s10853-006-0637-z.
- [9] Palomo, A., Grutzeck, M. W., & Blanco, M. T. (1999). Alkali-activated fly ashes: A cement for the future. *Cement and Concrete Research*, 29(8), 1323–1329. doi:10.1016/S0008-8846(98)00243-9.
- [10] Mustafa Al Bakria, A. M., Kamarudin, H., Bin Hussain, M., Khairul Nizar, I., Zarina, Y., & Rafiza, A. R. (2011). The effect of curing temperature on physical and chemical properties of geopolymers. *Physics Procedia*, 22, 286–291. doi:10.1016/j.phpro.2011.11.045.
- [11] Cheng, Y. hong, Huang, F., Liu, R., Hou, J. long, & Li, G. lu. (2016). Test research on effects of waste ceramic polishing powder on the permeability resistance of concrete. *Materials and Structures*, 49(3), 729–738. doi:10.1617/s11527-015-0533-6.
- [12] García-Ten, F. J., Quereda Vázquez, M. F., Gil Albalat, C., Chumillas Villalba, D., Zaera, V., & Segura Mestre, M. C. (2016). LIFE CERAM. Zero waste in ceramic tile manufacture. *Key Engineering Materials*, 663, 23–33. doi:10.4028/www.scientific.net/KEM.663.23.
- [13] El-Dieb, A. S., Taha, M. R., Kanaan, D., & Aly, S. T. (2018). Ceramic waste powder: From landfill to sustainable concretes. *Proceedings of Institution of Civil Engineers: Construction Materials*, 171(3), 109–116. doi:10.1680/jcoma.17.00019.
- [14] Sánchez de Rojas, M. I., Frías, M., Sabador, E., Asensio, E., Rivera, J., & Medina, C. (2018). Use of ceramic industry milling and glazing waste as an active addition in cement. *Journal of the American Ceramic Society*, 101(5), 2028–2037. doi:10.1111/jace.15355.
- [15] Huseien, G. F., Sam, A. R. M., Shah, K. W., & Mirza, J. (2020). Effects of ceramic tile powder waste on properties of self-compacted alkali-activated concrete. *Construction and Building Materials*, 236, 117574. doi:10.1016/j.conbuildmat.2019.117574.

- [16] Aly, S. T., Kanaan, D. M., El-Dieb, A. S., & Abu-Eishah, S. I. (2018). Properties of Ceramic Waste Powder-Based Geopolymer Concrete. *International Congress on Polymers in Concrete (ICPIC 2018)*, 429–435. doi:10.1007/978-3-319-78175-4\_54.
- [17] Rashad, A. M., & Essa, G. M. F. (2020). Effect of ceramic waste powder on alkali-activated slag pastes cured in hot weather after exposure to elevated temperature. *Cement and Concrete Composites*, 111, 103617. doi:10.1016/j.cemconcomp.2020.103617.
- [18] Zhang, G. Y., Bae, S. C., Lin, R. S., & Wang, X. Y. (2021). Effect of waste ceramic powder on the properties of alkali-activated slag and fly ash pastes exposed to high temperature. *Polymers*, 13(21). doi:10.3390/polym13213797.
- [19] Shoaiei, P., Musaei, H. R., Mirlohi, F., Narimani zamanabadi, S., Ameri, F., & Bahrami, N. (2019). Waste ceramic powder-based geopolymer mortars: Effect of curing temperature and alkaline solution-to-binder ratio. *Construction and Building Materials*, 227, 116686. doi:10.1016/j.conbuildmat.2019.116686.
- [20] Huseien, G. F., Sam, A. R. M., Shah, K. W., Mirza, J., & Tahir, M. M. (2019). Evaluation of alkali-activated mortars containing high volume waste ceramic powder and fly ash replacing GBFS. *Construction and Building Materials*, 210, 78–92. doi:10.1016/j.conbuildmat.2019.03.194.
- [21] Sarkar, M., & Dana, K. (2021). Partial replacement of metakaolin with red ceramic waste in geopolymer. *Ceramics International*, 47(3), 3473–3483. doi:10.1016/j.ceramint.2020.09.191.
- [22] Azevedo, A. R. G., Vieira, C. M. F., Ferreira, W. M., Faria, K. C. P., Pedroti, L. G., & Mendes, B. C. (2020). Potential use of ceramic waste as precursor in the geopolymerization reaction for the production of ceramic roof tiles. *Journal of Building Engineering*, 29. doi:10.1016/j.job.2019.101156.
- [23] Saxena, R., & Gupta, T. (2022). Assessment of mechanical, durability and microstructural properties of geopolymer concrete containing ceramic tile waste. *Journal of Material Cycles and Waste Management*, 24(2), 725–742. doi:10.1007/s10163-022-01353-5.
- [24] Memiş, S., & Bilal, M. A. M. (2022). Taguchi optimization of geopolymer concrete produced with rice husk ash and ceramic dust. *Environmental Science and Pollution Research*, 29(11), 15876–15895. doi:10.1007/s11356-021-16869-w.
- [25] Adak, D., Sarkar, M., & Mandal, S. (2017). Structural performance of nano-silica modified fly-ash based geopolymer concrete. *Construction and Building Materials*, 135, 430–439. doi:10.1016/j.conbuildmat.2016.12.111.
- [26] Nath, S. K., Maitra, S., Mukherjee, S., & Kumar, S. (2016). Microstructural and morphological evolution of fly ash based geopolymers. *Construction and Building Materials*, 111, 758–765. doi:10.1016/j.conbuildmat.2016.02.106.
- [27] Amran, Y. H. M., Alyousef, R., Alabduljabbar, H., & El-Zeadani, M. (2020). Clean production and properties of geopolymer concrete; A review. *Journal of Cleaner Production*, 251, 119679. doi:10.1016/j.jclepro.2019.119679.
- [28] Deb, P. S., Sarker, P. K., & Barbhuiya, S. (2015). Effects of nano-silica on the strength development of geopolymer cured at room temperature. *Construction and Building Materials*, 101, 675–683. doi:10.1016/j.conbuildmat.2015.10.044.
- [29] Parveen, Singhal, D., Junaid, M. T., Jindal, B. B., & Mehta, A. (2018). Mechanical and microstructural properties of fly ash based geopolymer concrete incorporating alccofine at ambient curing. *Construction and Building Materials*, 180, 298–307. doi:10.1016/j.conbuildmat.2018.05.286.
- [30] Albitar, M., Mohamed Ali, M. S., Visintin, P., & Drechsler, M. (2017). Durability evaluation of geopolymer and conventional concretes. *Construction and Building Materials*, 136, 374–385. doi:10.1016/j.conbuildmat.2017.01.056.
- [31] Naskar, S., & Chakraborty, A. K. (2016). Effect of nano materials in geopolymer concrete. *Perspectives in Science*, 8, 273–275. doi:10.1016/j.pisc.2016.04.049.
- [32] Wardhono, A., Gunasekara, C., Law, D. W., & Setunge, S. (2017). Comparison of long term performance between alkali activated slag and fly ash geopolymer concretes. *Construction and Building Materials*, 143, 272–279. doi:10.1016/j.conbuildmat.2017.03.153.
- [33] Shah, K. W., & Huseien, G. F. (2020). Bond strength performance of ceramic, fly ash and GBFS ternary wastes combined alkali-activated mortars exposed to aggressive environments. *Construction and Building Materials*, 251, 119088. doi:10.1016/j.conbuildmat.2020.119088.
- [34] IS-3812 (Part1). (2013). Indian Standard Pulverized Fuel Ash-Specification, Part 1 for Use as Pozzolana in Cement, Cement Mortar and Concrete (Third Revision). Bureau of Indian Standards, New Delhi, India.
- [35] El-Dieb, A. S., Taha, M. R., & Abu-Eishah, S. I. (2019). The use of ceramic waste powder (CWP) in making eco-friendly concretes. *Ceramic Materials: Synthesis, Characterization, Applications and Recycling*, 1-35. doi:10.5772/intechopen.81842.
- [36] Sathish Kumar, V., Ganesan, N., & Indira, P. V. (2017). Effect of Molarity of Sodium Hydroxide and Curing Method on the Compressive Strength of Ternary Blend Geopolymer Concrete. *IOP Conference Series: Earth and Environmental Science*, 80(1), 12011. doi:10.1088/1755-1315/80/1/012011.
- [37] IS-383. (2016). Indian Standard Coarse and Fine Aggregates for Concrete (Third Revision). Bureau of Indian Standards, New Delhi, India.

- [38] Lloyd, N., & Rangan, V. (2010). Geopolymer concrete with fly ash. The Second International Conference on sustainable construction Materials and Technologies, 28-30 June, 2010, Ancona, Italy.
- [39] IS-1199 (Part 2). (2018). Indian Standard Fresh Concrete-Methods of Sampling, Testing and Analysis, Part 2 determination of consistency of fresh concrete (first revision). Bureau of Indian Standards, New Delhi, India.
- [40] IS-516 (Part1-Sec1). (2021). Hardened Concrete-Methods of Test-Part1 Testing of Strength of Hardened Concrete-Section 1 Compressive, Flexural and Split tensile Strength. Bureau of Indian Standards, New Delhi, India.
- [41] IS-5816. (1999). Indian Standard Splitting tensile Strength of Concrete Method of Test (First revision). Bureau of Indian Standards, New Delhi, India.
- [42] ASTM C642-13. (2013). Standard Test Method for density, Absorption, and Voids in Hardened Concrete. ASTM International, Pennsylvania, United States.
- [43] IS-456. (2000). Indian Standard Plain and reinforced Concrete Code of Practice (Fourth Revision). Bureau of Indian Standards, New Delhi, India.
- [44] Sofi, M., van Deventer, J. S. J., Mendis, P. A., & Lukey, G. C. (2007). Engineering properties of inorganic polymer concretes (IPCs). *Cement and Concrete Research*, 37(2), 251–257. doi:10.1016/j.cemconres.2006.10.008.
- [45] Balamuralikrishnan, R., & Saravanan, J. (2021). Effect of addition of alccofine on the compressive strength of cement mortar cubes. *Emerging Science Journal*, 5(2), 155-170. doi:10.28991/esj-2021-01265.
- [46] Provis, J. L., & van Deventer, J. S. J. (2007). Geopolymerisation kinetics. 2. Reaction kinetic modelling. *Chemical Engineering Science*, 62(9), 2318–2329. doi:10.1016/j.ces.2007.01.028.
- [47] IS-10262. (2019). Indian Standard Concrete Mix proportioning-Guidelines (Second Revision). Bureau of Indian Standards, New Delhi, India.
- [48] Abdollahnejad, Z., Luukkonen, T., Mastali, M., Kinnunen, P., & Illikainen, M. (2019). Development of One-Part Alkali-Activated Ceramic/Slag Binders Containing Recycled Ceramic Aggregates. *Journal of Materials in Civil Engineering*, 31(2), 4018386. doi:10.1061/(asce)mt.1943-5533.0002608.
- [49] Shehata, N., Mohamed, O. A., Sayed, E. T., Abdelkareem, M. A., & Olabi, A. G. (2022). Geopolymer concrete as green building materials: Recent applications, sustainable development and circular economy potentials. *Science of the Total Environment*, 836, 155577. doi:10.1016/j.scitotenv.2022.155577.
- [50] Chindaprasirt, P., & Rattanasak, U. (2017). Characterization of the high-calcium fly ash geopolymer mortar with hot-weather curing systems for sustainable application. *Advanced Powder Technology*, 28(9), 2317–2324. doi:10.1016/j.appt.2017.06.013.
- [51] Amin, S. K., El-Sherbiny, S. A., El-Magd, A. A. M. A., Belal, A., & Abadir, M. F. (2017). Fabrication of geopolymer bricks using ceramic dust waste. *Construction and Building Materials*, 157, 610–620. doi:10.1016/j.conbuildmat.2017.09.052.
- [52] Vaidya, S., Diaz, E. I., & Allouche, E. N. (2011). Experimental evaluation of self-cure geopolymer concrete for mass pour applications. *World of Coal Ash (WOCA) Conference*, 9-12 May, 2011, Denver, United States.
- [53] Topark-Ngarm, P., Chindaprasirt, P., & Sata, V. (2015). Setting Time, Strength, and Bond of High-Calcium Fly Ash Geopolymer Concrete. *Journal of Materials in Civil Engineering*, 27(7). doi:10.1061/(asce)mt.1943-5533.0001157.
- [54] Lee, S., & Shin, S. (2019). Prediction on compressive and split tensile strengths of GGBFS/FA based GPC. *Materials*, 12(24), 4198. doi:10.3390/MA12244198.
- [55] Diaz-Loya, E. I., Allouche, E. N., & Vaidya, S. (2011). Mechanical properties of fly-ash-based geopolymer concrete. *ACI Materials Journal*, 108(3), 300–306. doi:10.14359/51682495.
- [56] Jindal, B. B., Jangra, P., & Garg, A. (2020). Effects of ultra-fine slag as mineral admixture on the compressive strength, water absorption and permeability of rice husk ash based geopolymer concrete. *Materials Today: Proceedings*, 32, 871–877. doi:10.1016/j.matpr.2020.04.219.
- [57] McCarter, W. J., Ezirim, H., & Emerson, M. (1992). Absorption of water and chloride into concrete. *Magazine of Concrete Research*, 44(158), 31–37. doi:10.1680/macr.1992.44.158.31.
- [58] Alexander, M. G., Mackechnie, J. R., & Ballim, Y. (1999). Guide to the use of durability indexes for achieving durability in concrete structures, Research Monograph No. 2. University of Cape Town, Department of Civil Engineering: Cape Town, South Africa.
- [59] Chen, X., Zhang, D., Cheng, S., Xu, X., Zhao, C., Wang, X., Wu, Q., & Bai, X. (2022). Sustainable reuse of ceramic waste powder as a supplementary cementitious material in recycled aggregate concrete: Mechanical properties, durability and microstructure assessment. *Journal of Building Engineering*, 52, 104418. doi:10.1016/j.job.2022.104418.
- [60] Alehyen, S., El Achouri, M., & Taibi, M. (2017). Characterization, microstructure and properties of fly ash-based geopolymer. *Journal of Materials and Environmental Science*, 8(5), 1783–1796.